IEICE TRANS. COMMUN., VOL.E85–B, NO.6 JUNE 2002

PAPER

Design of a Multi Beam Feed Using a Nonradiative Dielectric Rotman Lens

Jae-Gon LEE[†], **Jeong-Hae LEE**[†], *and* **Heung-Sik TAE**[††], ***Nonmembers***

SUMMARY In this paper, a rotman lens of multi-beam feed that can be applied to a car collision avoidance radar is designed using nonradiative dielectric (NRD) guide appropriate to the millimeter wave frequency. For the optimum condition, NRD guide at the transmission lines of input and output ports is designed to obtain low loss, small coupling between the transmission lines, and dominant mode operation. The rotman lens is also optimized so as to minimize sidelobe of array factor. To prevent beam pattern from being distorted, multiple-reflection from sidewall has been eliminated by corrugated sidewall.

key words: *nonradiative dielectric (NRD), rotman lens, multi-beam feed*

1. Introduction

Multi-beam feed which can be applied to a car collision avoidance radar [1], [2] in the millimeter wave frequency has been studied in this paper. A car collision avoidance radar requires minimum beams of three because of detecting distance, ascertaining velocity, and distinguishing obstacle in the main, left, and right lane, respectively. There are various multi-beam feeds [3] such as maxon-blass matrix, butler matrix, ruze lens, and rotman lens. Maxon-blass matrix, consisting of M input ports and N output ports, is neither economical nor compact since it requires M × N directional couplers. Butler matrix also requires many couplers and phase shifters. In addition, it is hard to be implemented by a planar structure because it needs many non-intersecting crossovers of multi-layer. Ruze lens is not suitable for car collision avoidance radar since it is composed of two beams. Therefore, a rotman lens [4] can be one of the promising candidates for multi-beam feed of car collision avoidance radar. It has input ports of the same number of beams and plenty of output ports and then forms to obtain beam of intending angle at each input port.

A rotman lens can be made of parallel plate or microstrip. However, its volume is bulky when it is designed with parallel plate. Moreover, if we had used microstrip in a rotman lens [5], we would encounter a difficulty situation of low beam gain due to high conduction loss in the millimeter wave frequency of 77 GHz. In this paper, a rotman lens with nonradiative dielectric (NRD) guide [6] has been proposed to realize a compact size and a low loss of beam feed at 77 GHz. While NRD guide has characteristic of low loss in the millimeter wave band, it has a relatively strong coupling characteristic compared to microstrip [7]. Thus, coupling between NRD guide output ports of rotman lens may give rise to distortion of beam pattern. These coupling effects should be taken into account in the design of NRD rotman lens. Besides coupling between the transmission lines of input and output ports, multiple-reflection from sidewall, which occurs due to structural characteristic, causes distortion of output beam. To eliminate multiple-reflection, the sidewall of rotman lens has been corrugated for matching. Finally, the rotman lens is optimized to minimize sidelobe by computing its array factor.

2. Loss, Coupling and Operation of Dominant Mode of NRD Guide

The structure of NRD guide is shown in Fig. 1. It consists of parallel-plate guide with a dielectric strip inserted between the plates. Structurally, it is identical to the H-guide except that the plate separation ($a \leq \lambda/2$) is less than half the free space wavelength. Thus, the field of guided wave is bound within a dielectric strip and decays exponentially away from a dielectric strip, resulting in nonradiative mode.

In this paper, a dominant mode of LSM_{11}, whose electric field is predominantly parallel to conductor strips, has been utilized to prevent TEM mode, whose electric field is vertical to conductor strips, from being excited inside a lens region as well as to obtain

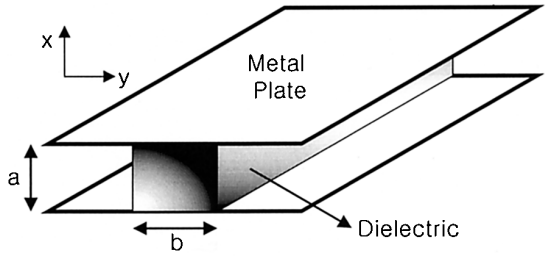

Fig. 1 Structure of NRD guide.

Manuscript received August 1, 2001.
Manuscript revised January 15, 2002.

[†]The authors are with the Dept. of radio science and communication engineering, The Hongik University, Seoul, South Korea.
[††]The author is with the School of Electronic and Electrical Engineering, The Kyungpook National University, Taegu, South Korea.

Table 1 Comparison of transmission loss of NRD guide and microstrip versus millimeter wave frequency (dielectric constant = 2.08, loss tangent = 0.0004, conductivity = 5.813×10^7 (S/m), Thickness of microstrip = 0.127 mm, line width of microstrip = 0.112 mm, dielectric of NRD guide = width (1.75 mm), height (1.77 mm)).

	Loss	Frequency		
		70GHz	80GHz	90GHz
NRD	Conduction (dB/λ)	0.0362	0.0155	0.0085
	Dielectric (dB/λ)	0.0416	0.0249	0.0206
	Total (dB/λ)	0.0778	0.0404	0.0291
	Loss	Frequency		
		70GHz	80GHz	90GHz
Micro-strip	Conduction (dB/λ)	0.2332	0.2143	0.2018
	Dielectric (dB/λ)	0.0261	0.0263	0.0265
	Total (dB/λ)	0.2593	0.2466	0.2283

low transmission loss [6]. Otherwise, an excited TEM mode inside a lens might cause a leakage since it has no cutoff characteristic. The propagation constant of LSM mode is simply defined as [8]

$$\beta = \sqrt{\epsilon_r k_0^2 - k_x^2 - k_{y1}^2} = \sqrt{k_0^2 - k_x^2 - k_{y2}^2} \tag{1}$$

where k_{y1} and k_{y2} are the propagation and attenuation constant in the inside and outside dielectric, respectively. Note that $k_x = m\pi/a$ and $k_0 = \omega/c$. Also, k_{y1} and k_{y2} are related by

$$k_{y1} \tan\left(\frac{k_{y1} b}{2}\right) = \epsilon_r k_{y2}. \tag{2}$$

To validate a use of NRD guide for obtaining low transmission loss, transmission losses of NRD guide and microstrip are calculated [9], [10] and compared in Table 1. To compare loss of NRD guide with that of microstrip, it is assumed that a dielectric of NRD guide and microstrip is made up of the same dielectric (Teflon) and conductor (copper). Dielectric constant and loss tangent of Teflon are assumed to be 2.08 and 0.0004, respectively. Conductivity of copper is 5.813×10^7 (S/m). Table 1 shows that total transmission loss of NRD guide is much smaller than that of microstrip in the millimeter wave frequency due to a low conduction loss of NRD guide even though dielectric loss of NRD guide is comparable to that of microstrip. When a focal length of rotman lens, which will be decided later in this paper, is $16\lambda_g$ at 77 GHz, total loss of NRD lens is decreased by 80% compared with that of microstrip lens.

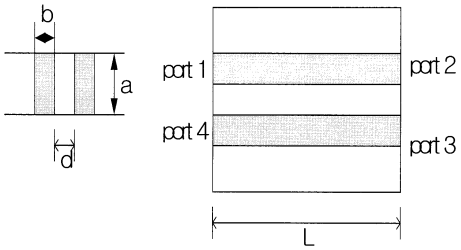

Fig. 2 Front and top view of two NRD guides model used to computation of a coupling.

To decide the dimension of cross section of NRD guide at the input and output ports of rotman lens, transmission loss is computed with respect to height and width of dielectric strip [8]. The computation results show that loss of transmission line decrease with height of dielectric strip. A loss of transmission line is relatively insensitive to width of dielectric strip. It is easy to conclude that larger value of height of dielectric strip results in a low loss of transmission line.

Figure 2 shows a front and top view of two NRD guides to investigate coupling between NRD output ports which would cause serious distortion of output beam pattern. A coupling coefficient between NRD guides is computed using the following Eqs. (3), (4) given by [7]

$$C = K \exp(-k_{y2} d) \tag{3}$$

$$K = \frac{\epsilon_r k_{y1}^2 k_{y2}^2}{\beta[(k_{y1}^2 + (\epsilon_r k_{y2}^2)^2)(\frac{k_{y2} b}{2}) + \epsilon_r (k_{y1}^2 + k_{y2}^2)]} \tag{4}$$

Note that Eq. (3) is approximate numerical formula which is valid when the value of d/λ_0 is larger than 0.1 in this calculation. Figure 3 and Fig. 4 show that coupling decreases with the distance between NRD guides as expected. The coupling between NRD guides as well as the transmission loss depends on the dimension of a cross section of NRD guide. As shown in Fig. 3 and Fig. 4, the larger values of width (b) and dielectric constant (ϵ_r) produce a smaller coupling since the fields are well confined in a dielectric. However, these larger values are limited by dominant mode (LSM_{11}) operation condition. It is also noted that coupling is relatively insensitive to height of dielectric.

The calculation results of Table 1, Fig. 3, and Fig. 4 are plotted in Fig. 5 for deciding the cross section dimension of NRD guide to obtain low loss and small coupling. As shown in Fig. 5, the possible values of a and b should be inside dotted lines for a single LSM_{11}

mode operation. Loss decreases with height of dielectric. Coupling decreases and loss is almost flat with width of dielectric. Thus, the values of a and b are $0.5\lambda_0$ and $0.74\lambda_0/\sqrt{\epsilon_r - 1}$ for the lowest loss and smallest coupling, respectively. However, these values are too marginal for a single mode operation since the values are located on the dotted lines in Fig. 5. Therefore, the values of a and b are chosen as $0.45\lambda_0$ and $0.7\lambda_0/\sqrt{\epsilon_r - 1}$, respectively, for low loss and small coupling under the condition of a single mode operation.

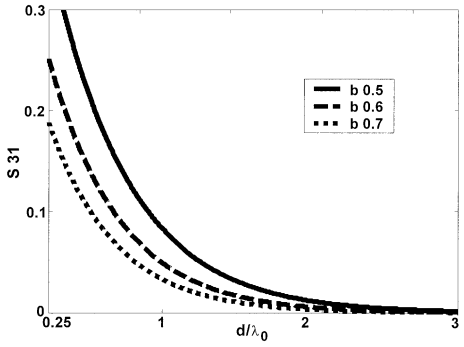

Fig. 3 Comparison of S_{31} versus width of dielectric strip (frequency=77 GHz, $a = 0.45\lambda_0$, $b = (0.5 \sim 0.7)\lambda_0/\sqrt{\epsilon_r - 1}$, dielectric constant=2).

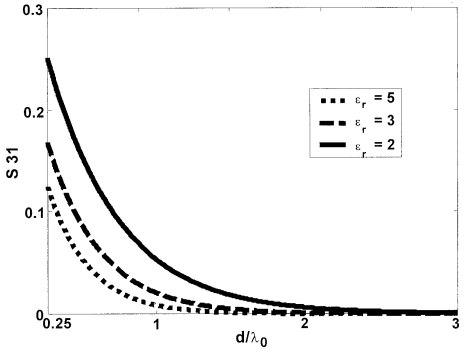

Fig. 4 Comparison of S_{31} versus dielectric constant (frequency=77 GHz, $a = 0.45\lambda_0$, $b = 0.6\lambda_0/\sqrt{\epsilon_r - 1}$, dielectric constant=2,3,5).

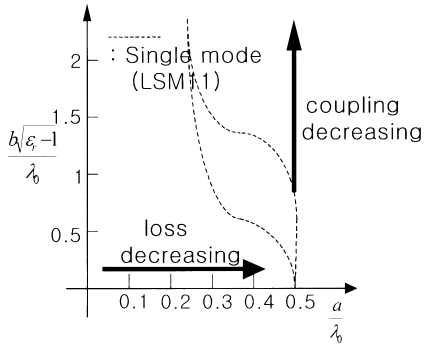

Fig. 5 Characteristics of NRD with its dimension when dielectric constant is 3.78.

3. Design of a Rotman Lens

A schematic diagram of rotman lens is illustrated in Fig. 6. An NRD rotman lens, which is proposed in this paper, is composed of three input ports to obtain three output beams. The beam is focused to array output ports provided that incident wave propagates to focal point. In order to steer an output beam with an angle of ψ in rotman lens, the path difference between two output rays from the point F_1 should satisfy Eq. (5) [3]. Similarly, Eqs. (6) and (7) should be satisfied to steer an output beam with an angle of $-\psi$ and 0°, respectively.

$$\vec{F_1P}\sqrt{\epsilon_{eff}} + W + N\sin\psi = F\sqrt{\epsilon_{eff}} + W_0 \tag{5}$$

$$\vec{F_2P}\sqrt{\epsilon_{eff}} + W - N\sin\psi = F\sqrt{\epsilon_{eff}} + W_0 \tag{6}$$

$$\vec{GP}\sqrt{\epsilon_{eff}} = G\sqrt{\epsilon_{eff}} + W_0 \tag{7}$$

Note that the path lengths such as F_1P, F_2P, GP, and G should be multiplied by the value of $\sqrt{\epsilon_{eff}}$ in Eqs. (5), (6), and (7), respectively, since incident wave propagates through dielectric medium instead of free space which results in longer electric path length. Furthermore, since LSM_{11} mode in NRD guide is incident on a rotman lens, TE mode is generated inside a lens. Thus, ϵ_{eff} is given by Eq. (8)

$$\sqrt{\epsilon_{eff}} = \lambda_0/\lambda_g \tag{8}$$

where λ_0 and λ_g are free space wavelength and TE mode wavelength, respectively [11].

An NRD rotman lens can be designed with the following equation [12] with the modified Eqs. (5), (6), (7), and (8)

$$a\omega^2 + b\omega + c = 0 \tag{9}$$

where

$$a = 1 - \frac{(1-\beta)^2}{(1-\beta C)^2} - \frac{\zeta^2}{\beta^2}$$

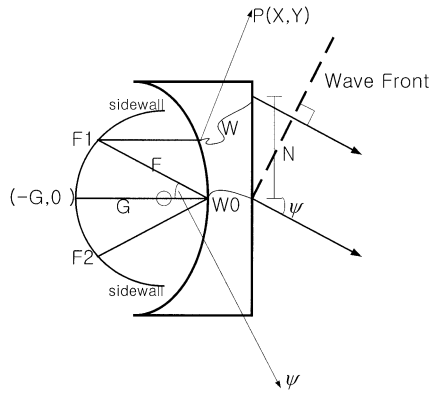

Fig. 6 Schematic diagram of a rotman lens.

$$b = -2 + \frac{2\zeta^2}{\beta} + \frac{2(1-\beta)}{1-\beta C} - \frac{\zeta^2 S^2(1-\beta)}{(1-\beta C)^2}$$
$$c = -\zeta^2 + \frac{\zeta^2 S^2}{1-\beta C} - \frac{\zeta^4 S^4}{4(1-\beta C)^2}$$
$$\omega = \frac{W - W_0}{G\sqrt{\epsilon_r}}$$
$$\beta = \frac{F}{G}$$
$$\zeta = \frac{N\gamma}{G\sqrt{\epsilon_r}}$$
$$\gamma = \frac{\sin\psi}{\sin\alpha}$$
$$C = \cos\alpha$$
$$S = \sin\alpha.$$

The value of ω is determined by solving Eq. (9). Then, the position (X, Y) and length (W) of output ports are computed to Eqs. (10) and (11).

$$X = \frac{(\zeta^2 S^2 - 2\beta\omega + 2\omega)G}{2(\beta C - 1)}, \quad Y = \zeta\left(1 - \frac{\omega}{\beta}\right)G \tag{10}$$

$$\omega = \frac{W - W_0}{G\sqrt{\epsilon_r}} \tag{11}$$

Note that W_0 is the length of transmission line of the center output port.

One example of designed layout of rotman lens with three input and 29 output ports is illustrated in Fig. 7. The flat dielectric structure with a thickness of a ($\leq \lambda/2$) in Fig. 7 is sandwiched between the parallel conductor plates. The corrugated sidewall for matching which will discussed in the next section is also shown. Note that the input and output ports consist of NRD guide with thickness of a. The ports are connected to a rotman lens with a tapered section for matching purpose.

To optimize an NRD rotman lens which has a minimum side lobe, array factor is computed using 2-D green function [13] based on far-field approximation and 2-D Friis transmission equation after port position and length of output transmission line are determined.

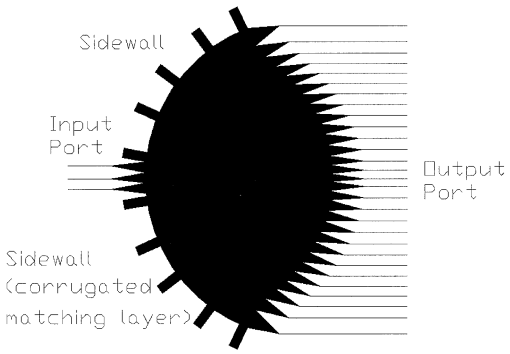

Fig. 7 Structure of a rotman lens.

Then, a electric field of internal parallel plate is given by Eqs. (12) and (13) using 2-D green function.

$$E(\rho, \theta) = E_0 D\sqrt{\frac{k}{2\pi\rho}}\tilde{E}(D, \theta) \tag{12}$$

$$\tilde{E}(D, \theta) = \frac{\cos\theta + \cos\theta_i}{2}\frac{\sin\left(\frac{kD}{2}(\sin\theta - \sin\theta_i)\right)}{\frac{kD}{2}(\sin\theta - \sin\theta_i)} \cdot \exp\left(-jk\rho + j\frac{\pi}{4}\right) \tag{13}$$

where (ρ, θ) is observation point inside lens and D is opening width of tapered output port. ρ_{ij}, ρ_c, and k_c are distance between i-th input port and j-th output port, length of output transmission line, and wave number of considering effective permittivity in the transmission line, respectively. A transmission coefficient between input and output port can be derived from 2-D Friis transmission equation. Including ρ_{ij} and ρ_c, complex transmission coefficient from i-th input port to j-th output port is derived as Eq. (14).

$$S_{ij} = \sqrt{\frac{kD_jD_i}{2\pi\rho}}\tilde{E}_j(D_j, \theta_j)\tilde{E}_i(D_i, \phi_i) \cdot \exp(-j(k\rho_{ij} + k_c\rho_c)) \tag{14}$$

Then, array factor (AF) is represented by

$$AF = |\Sigma C_i \exp(ja_i + jk_0\vec{a_r} \cdot \vec{r_i})| \tag{15}$$

where C_i and a_i is magnitude and phase of Eq. (14). $\vec{a_r}$ and $\vec{r_i}$ is unit vector of observation point and position vector of source point, respectively.

Array factor is optimized through flow chart shown in Fig. 8. In this paper, structural parameters for optimization are array spacing, focal length, and focal ratio to obtain minimum sidelobe level. It is true that the number of ports determines half power beam width (HPBW) of the array, i.e., HPBW is getting smaller as

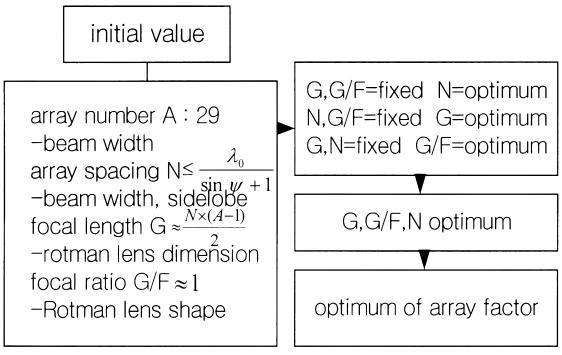

Fig. 8 Flowchart for optimization of array factor to obtain minimum sidelobe.

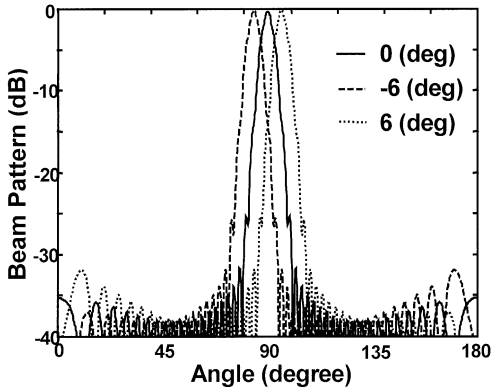

Fig. 9 Optimized array factor.

Table 2 Dimensions of an optimized NRD rotman lens.

Frequency (77GHz)			
Rotman lens	**N**	**G**	**G/F**
	3mm	$16\lambda_g$	0.997
Transmission line	**a**	**b**	ε_r
	$0.45\ \lambda_0$	$0.7\lambda_0/\sqrt{\varepsilon_r - 1}$	3.78

the number of ports increases. Since we do not have a concrete requirement for HPBW at this time, we choose the number of ports is 29 and used it as an initial value as indicated in Fig. 8. The calculation result shows that beam width increases in proportion to focal ratio and in inverse proportion to array spacing. A sidelobe level increases in proportion to array spacing. Focal length relates with only dimension of rotman lens. Repeating the calculation according to the flow chart shown in Fig. 8, optimum of array factor is obtained as shown in Fig. 9. The amplitude difference between main beam and sidelobe is 34 dB. The dimensions of NRD rotman lens for optimized array factor is shown in Table 2.

4. Corrugated Sidewall

To consider multiple-reflection from sidewall which would cause distortion of beam pattern, an NRD rotman lens is simulated using High Frequency Structure Simulator (HFSS Ver. 6) since a 2-D green function does not include multiple reflection. However, it is almost impossible to simulate the structure in Fig. 7, which has 3 input ports and 29 output ports, using HFSS since it requires tremendous computing time and memory. Thus, an NRD rotman lens with one input port and five output ports is simulated to test the effects of corrugated sidewall as shown in Fig. 10.

One difficult problem in this simulation is that only one single mode of LSM_{11} cannot be excited at the NRD input port. LSE_{11} mode is always generated together with LSM_{11} mode since LSE_{11} mode has a

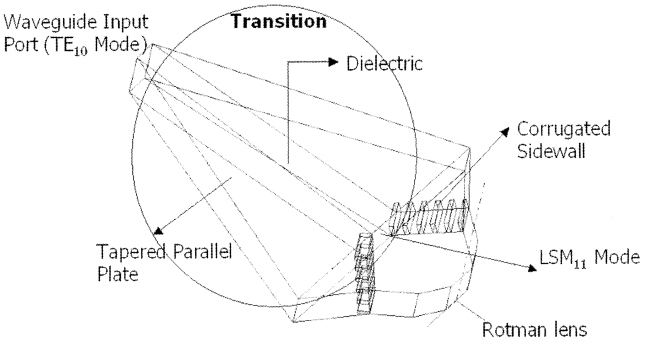

Fig. 10 Rotman lens with one input port and five output ports.

lower cutoff frequency than LSM_{11} mode. This makes it difficult to interpret our simulation result. To circumvent this problem, a transition to excite only LSM_{11} mode is employed as shown in Fig. 10. The input port of the transition is the dielectric filled-waveguide operated with TE_{10} mode. Then, the electric field parallel to flared parallel plate is launched to input of rotman lens since cross section of rectangular waveguide rotates with 90 degrees. Thus, the parallel electric field is converted with LSM_{11} mode at input port of rotman lens since the electric filed of LSM_{11} is parallel to conducting plate as shown in Fig. 10. On the other hand, LSE_{11} mode is not excited since its electric filed is vertically polarized. The simulated transmission coefficient of the transition, as expected, is one above cutoff frequency of LSM_{11} mode and the electric field is parallel to conducting plates. To remove the effects of the cutoff characteristic of waveguide, the cross section dimension of rectangular waveguide is determined for its cutoff frequency to be lower than that of LSM_{11} mode.

Figure 11 shows the result of simulation. The transmission coefficients from center input port to five output ports are simulated with and without corrugated sidewall, respectively. Transmission coefficients are also calculated using 2-D green function which does not include multiple-reflection. The results with corrugated sidewall is closer to those from 2-D green function, indicating that corrugated sidewall eliminates multiple-reflection.

5. Characteristics of a Designed NRD Rotman Lens

In this section, the characteristics of a designed NRD rotman lens in the previous sections have been summarized. The sizes and losses of three types of rotman lens, i.e., parallel plate rotman lens, NRD rotman lens, and microstrip rotman lens have been compared in Table 3. For parallel plate rotman lens, the areas have been calculated for TEM, TE, and TM mode, respectively, since the areas depend on the wavelength in parallel plate. As shown in Table 3, an NRD rotman lens has

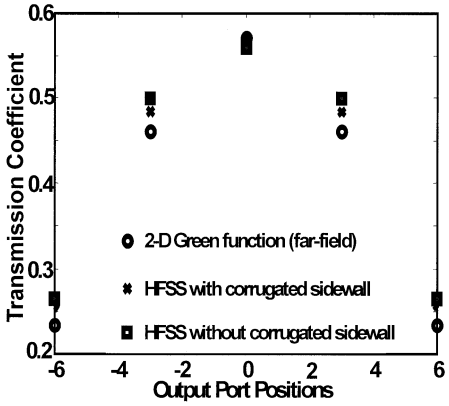

Fig. 11 Comparison of transmission coefficients (number of output=5, distance between output ports (N) = 3 mm).

Table 3 Comparison of size and loss of parallel plate, NRD, and microstrip rotman lens (frequency = 77 GHz, dielectric constant = 3.78, loss tangent = 0.0004, conductivity = 5.813×10^7 (S/m), skin depth = 2.088×10^{-6} m, line width of microstrip = 0.112 mm, number of input (output) ports = 3 (29), dielectric of NRD guide (width = 1.63 mm, height = 1.75 mm), focal length = $16\lambda_g$, focal ratio = 0.997, array spacing = 3 mm).

	Parallel plate rotman lens	NRD rotman lens	Microstrip rotman lens
Size of rotman lens (mm)	TE, TM 99.36×48 (4769mm^2) TEM 62.2×40 (2488 mm^2)	LSM (TE) 51.2×40 (2048 mm^2)	TEM 32×38 (1216 mm^2)
Loss (dB/ λ)	TE, TM 0.0015 TEM 0.0004	LSM (TE) 0.032	TEM 0.249

smaller volume than parallel plate rotman lens and less loss than microstrip rotman lens. The area of NRD rotman lens is decreased by 18% compared with that of parallel plate with TEM mode operation for dielectric constant of 3.78 in this paper. It is certain that the area of an NRD rotman lens can be further reduced if a dielectric of high dielectric constant is employed. Even though microstrip rotman lens has the smallest area among them, it has a very large conduction loss in the millimeter wave frequency as shown in the Table 3.

Coupling level is parameterized with respect to distance of d between output NRD guides. The array factor has been calculated by including coupling effects between NRD output ports. The array factor is calculated using Eq. (15) by adding S_{31} obtained from Eq. (3) to magnitude of C_i in Eq. (15). In this calculation, it is assumed that the phase of S_{31} is in phase with that of S_{ij} in Eq. (14). Thus, this estimation generates the worst distortion of the array factor. When optimized distance between output ports is 3 mm, the worst distorted sidelobe level is −19 dB. If this level is not enough for application, it could be improved by increasing d as shown in Table 4.

As discussed before, the transmission coefficents with corrugated side wall are closer to those from 2-D green function. This indicates that the corrugated sidewall eliminates multiple reflection since a 2-D green fuction does not include the multiple reflection. To be confirmed, the array factor has been calculated using the transmission coefficients in Fig. 11. The results shows that the sidelobe levels from 2-D green function, with and without corrugated sidewall are −17.1 dB, −11.6 dB, and −5.8 dB, respectively. This clearly indicates that corrugated sidewall eliminates multiple reflection.

Table 4 S_{31} and side-lobe level versus distance between transmission lines.

d (mm)	S_{31}	Side-Lobe Level
2	0.15	-14 (dB)
3	0.06	-20 (dB)
4	0.02	-25 (dB)
5	0.005	-32 (dB)

6. Conclusion

In this paper, a rotman lens of multi-beam feed that can be applied to a car collision avoidance radar in the frequency of 77 GHz is proposed and designed using low loss NRD guide. Since coupling between the NRD output ports gives rise to distortion of beam pattern, these coupling effects has been taken into account in the design of an NRD rotman lens. Besides coupling between the output ports, multiple-reflection from sidewall, which occurs due to structural characteristic, causes distortion of output beam. To eliminate multiple-reflection, the sidewall of a rotman lens has been corrugated. Furthermore, the NRD rotman lens are optimized so as to minimize sidelobe of array factor.

Acknowledgement

This work was supported by LG Innotek and grant No.2000-1-30200-009-3 from the basic Research Program of the Korea Science and Engineering Foundation.

References

[1] T. Yoneyama, "Millimeter-wave research activities in Japan," IEEE Trans. MTT, vol.46, no.6, pp.727–733, 1998.
[2] T. Tanizaki, H. Nishida, T. Nishiyama, H. Yamada, K. Sakamoto, and Y. Ishikawa, "Multi-beam automotive radar front end using non-contact cylindrical NRD switch," IEEE MTT-S Symposium Digest, vol.2, pp.521–524, 1998.
[3] Y.T. Lo and S.W. Lee, Antenna handbook, Ch.17, Ch.19, ITP, 1993.
[4] W. Rotman and R.F. Tuner, "Wide-angle microwave lens for line source applications," IEEE Trans. Antennas & Propag., vol.11, pp.623–632, Nov. 1963.

[5] S.F. Peik and J. Heinstadt, "Multiple beam microstrip array fed by rotman lens," IEEE AP, Ninth International Conference, vol.1, pp.348–351, 1995.
[6] T. Yoneyama and S. Nishida, "Nonradiative dielectric waveguide for millimeter-wave integrated circuits," IEEE Trans. MTT, vol.29, no.11, pp.1188–1192, 1981.
[7] T. Yoneyama, N. Tozawz, and S. Nishida, "Coupling characteristics of nonradiative dielectric waveguides," IEEE Trans. MTT, vol.31, no.8, pp.648–654, 1983.
[8] J. Dallaire and K. Wu, "Complete characterization of transmission losses in generalized NRD waveguide," IEEE Trans. MTT, vol.48, no.1, pp.121–125, 2000.
[9] S.K. Koul, Millimeter wave and optical dielectric integrated guides and circuits, Ch.6, John Wiley & Sons, 1997.
[10] D.M. Pozar, Microwave engineering, Ch.4, Addison Wesley, 1993.
[11] J.G. Lee, J.H. Lee, and H.S. Tae, "Design of a nonradiative dielectric rotman lens in the millimeter wave frequency," IEEE MTT-S Symposium Digest, vol.1, pp.551–554, Phoenix USA, May 20–25, 2001.
[12] R. Benjamin and A.J. Seeds, "Optical beam forming techniques for phased array antennas," IEE Proc., vol.139, no.6, pp.526–534, Dec. 1992.
[13] M.S. Smith and A.K.S. Fong, "Amplitude performance of Ruze and Rotman lens," The Radio and Electronic Engineer, vol.53, no.9, pp.329–336, Sept. 1983.

Jae-Gon Lee was born in 1977. He received the B.S. and M.S. degrees in the department of radio science and communication engineering in 1999 and 2001, respectively, from Hongik University, Korea. He is currently working toward the Ph.D. degree in Hongik University. His current research interests include the microwave/millimeter wave circuit.

Jeong-Hae Lee was born in 1962. He received the B.S. and M.S. degrees in Electrical Engineering in 1985 and 1988, respectively, from Seoul National University, Korea and the Ph.D. degree in Electrical Engineering in 1996 from University of California, Los Angeles, USA. From 1993 to 1996, he was a visiting scientist of General Atomics, San Diego, USA, where his major research was to develop the millimeter wave diagnostic system and to study the plasma wave physics. Since 1996, he has been at Hongik University, Seoul, Korea, where he is an assistant professor of department of radio science and communication engineering. His current research interests include the microwave/millimeter wave circuits and measurements. Dr. Lee is a member of IEEE.

Heung-Sik Tae received the B.S. degree from the Department of Electrical Engineering, Seoul National University, Seoul, Korea, in 1986 and M.S. degree and Ph.D. in Plasma Engineering from Seoul National University in 1988 and 1994, respectively. Since 1995, he has been as associate professor in the School of Electronic and Electrical Engineering, Kyungpook National University in Daegu, Korea. His research interests include the optical characterization and driving circuit of plasma display panel, the design of millimeter wave guiding structure, and MEMS or thick-film processing for millimeter wave device. Dr. Tae is a member of IEEE.